FREQUENCY-SHIFT KEYING (FSK) MODULATOR USING A MEMS SWITCH

Brad R. Jackson and Carlos E. Saavedra

Department of Electrical and Computer Engineering
Queen's University, Kingston, Ontario, Canada, K7L 3N6

brad.jackson@ece.queensu.ca carlos.saavedra@queensu.ca

ABSTRACT

In this paper, a new frequency-shift keying (FSK) modulator circuit is demonstrated that uses a single-pole double-throw MEMS switch to select between one of two resonators with different resonant frequencies. By controlling the state of the switch with the digital baseband data FSK modulation can be achieved. The circuit topology was tested using a packaged MEMS switch on a microwave hybrid printed circuit board. Measured results show output frequencies of 1.8 GHz and 1.9 GHz when the switch is in each of its states. The output power is 9.9 dBm at 1.8 GHz and 8.45 dBm at 1.9 GHz and the phase noise was measured to be -99 dBc and -98 dBc at a 1 MHz offset for the 1.8 GHz and the 1.9 GHz outputs, respectively.

1. INTRODUCTION

The monolithic or hybrid integration of microelectronic devices with microelectromechanical systems (MEMS) is opening new possibilities for microsystems that are very versatile. For instance, the front-end of a microwave communications transceiver can contain several MEMS devices. Well-known applications of MEMS include the use of switches for connecting the antenna to either the transmit and receive signal paths, tunable or reconfigurable MEMS bandpass filter to allow for frequency re-use of the transceivers, tank resonators, and phase shifters [1-3].

More recently, new applications have been suggested for MEMS devices such as binary phase shift keying (BPSK) modulators [4]. In this paper, we experimentally demonstrate the use of a MEMS switch in a frequency-shift keying (FSK) modulator. This paper is organized as follows: Section II describes the concept, Section III discusses the MEMS switch used, Sections IV and V are devoted to the oscillator and modulator design, Section VI and VII present the simulated and experimental results, and Section VIII concludes the work.

2. FSK MODULATOR CONCEPT

The concept of the proposed FSK modulator can be explained with aid of the block diagram in Figure 1. This figure shows a two-port transistor oscillator circuit with two separate tuning networks. The selection of one of the two tuning networks is performed by the single-pole double-throw (SPDT) MEMS switch, which is controlled by the digital baseband signal. By changing the tuning network that is connected to the rest of the oscillator, the frequency of oscillation can be changed in accordance with the digital data, thus producing FSK modulation. In most VCOs the tunable component is a varactor with a limited tuning range, and therefore the change in oscillation frequencies is usually small. In contrast, the proposed modulator is not limited by the variability of a single component, and as such, this topology could be used for an application where the two oscillation frequencies differ significantly. The oscillator configuration and its resonator structures can theoretically be implemented using any method or technology desired with the proposed topology.

A potential application of the topology shown in Figure 1, in addition to an FSK modulator, is as a local oscillator that can operate at two completely different frequencies. This could potentially enable a transceiver to operate at two significantly different frequency bands, thus adding functionality to a system without significantly increasing the size or complexity of the circuitry. Tunable

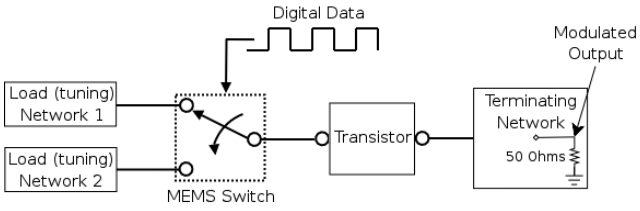

Figure 1: Proposed FSK modulator block diagram

filters would also be required if the Figure 1 topology was used for this application. A MEMS-based tunable bandpass filter that could be used for this purpose is presented in [5] where a SPDT MEMS switch is used to select between two bandpass filters with different centre frequencies.

3. MEMS SWITCH

RF MEMS switches in general have excellent high-frequency performance with low insertion losses and high isolation. A great number of RF MEMS switches have been reported over the last decade, some of which have demonstrated insertion losses of less than 0.1 dB and isolations greater than 30 dB up to 40 GHz and higher. In addition, MEMS switches are extremely linear devices with very low intermodulation products. In fact, their third-order intercept point performance is approximately 30 dB greater than PIN diodes or FET switches. Furthermore, they can be designed to consume essentially zero current, depending on the actuation mechanism, which can lead to extremely low power consumptions (e.g. 10 – 100 nJ per switching cycle for electrostatically actuated switches). Since MEMS switches can be manufactured using integrated circuit techniques, there is also the potential for considerable cost savings if the devices are produced in large quantities. Currently there is very good understanding of the theory and operation of MEMS switches, and their potential has been discussed and demonstrated at length in the literature. However, given that the technology is relatively new, there are still several issues with RF MEMS switches that are currently being investigated. First, the fastest MEMS switches to date have a switching time of about 1 μs and most MEMS switches are considerably slower than this which may rule out their use in certain applications. Given the mechanical nature of the switches, these devices will find applications in areas where switching speed is not a limiting factor, such as reconfigurable antennas, phase shifters, filters, and low data-rate communications systems, to name a few. The power handling capabilities of MEMS switches is not as high as in PIN diodes or FETs, although advances in this regard have been made recently where MEMS switches are demonstrated to operate up to 5.5 W [6]. The reliability of MEMS switches, or the Mean-Time-To-Failure (MTTF), has been constantly improving and many switches are already reaching 100 billion (10^{11}) cycles.

The MEMS switch used for the FSK modulator in this work is a packaged magnetically actuated single-pole double-throw (SPDT) latching switch made by Magfusion [7]. The main advantage to using this switch is the relatively low actuation voltages that are required. It is not uncommon for electrostatically actuated switches to have actuation voltages between 50 and 100 V, which can make integration with the other electronic circuitry challenging. With this switch, much more easily attained actuation voltages of only ±5 V are required. The theory behind this switch, and measured performance will be discussed below.

3.1. Theory of Operation

The operational concept of the Magfusion MEMS switch, first published in [8], is based on the preferential magnetization of a permalloy cantilever in a static external magnetic field. The cantilever can have either a clockwise or counterclockwise torque in a uniform magnetic field depending on the orientation of the magnetization along the beam. The ability for the switch to latch is due to the presence of a permanent permalloy magnet beneath the substrate. The magnetic field produced by this magnet holds the cantilever in a constant position until a change in state occurs. To change the state of the switch, a pulse of current is sent through a coil beneath the cantilever which essentially overpowers the permanent magnet's field and realigns the magnetization of the cantilever. This reverses the torque on the beam and causes it to change states. Figure 2 shows the top view of the latching relay.

A simplified schematic of the Magfusion SPDT switch is given in Figure 3. By changing the direction of the current through the coil the state of the switch can be changed. The control pulse that is required to change the state of the switch is approximately 100 mA, which

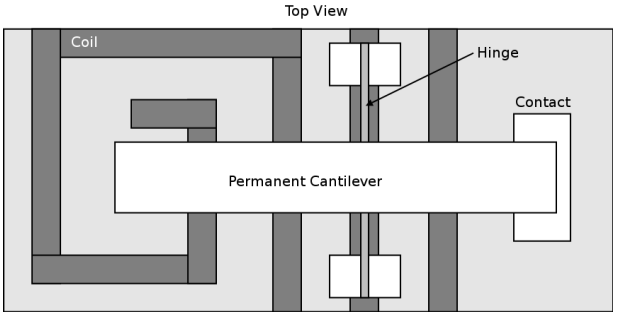

Figure 2: Top view of hinged latching relay (after [4])

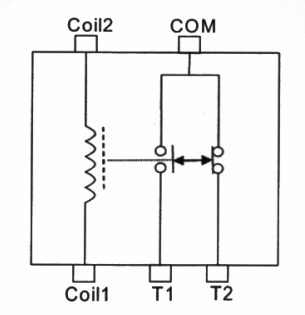

Figure 3: SPDT MEMS switch schematic [3]

corresponds to control voltages of ±5 V since the typical coil resistance is about 50 Ω. The time it takes for the switch to change states is approximately 100 μs, which means the maximum switching frequency is about 5 kHz. Due to the magnetic actuation of this switch that is based on applying current pulses, its power consumption may be higher than other MEMS switches that have different actuation mechanisms (e.g. electrostatic). However, this switch has zero quiescent power dissipation because it will stay magnetically latched indefinitely until another control pulse is applied.

3.2. Measured Performance

The performance of the Magfusion MEMS switch was measured using the same substrate to be used for the proposed MEMS-based FSK modulator. A printed circuit board (PCB) was fabricated and the packaged switch was fixed to it. S-parameter measurements were performed using an Agilent 8510C vector network analyzer with no gating and a full two-port calibration was performed prior to measurements. An Anritsu universal test fixture (model: 3680-20) was used to connect the coaxial cables from the network analyzer to the microstrip traces on the circuit board. Shown in Figure 4 is the measured insertion loss of the switch from 1 GHz to 4 GHz. In the 2 GHz range, the insertion loss is approximately 0.5 dB, and it is less than 1 dB up to 4 GHz. The isolation is shown in Figure 5 to be less than -30 dB up to 4 GHz, and the input return loss shown in Figure 6 is less than -10 dB up to 4 GHz. These results match the circuit board-level results reported by the manufacturer quite closely.

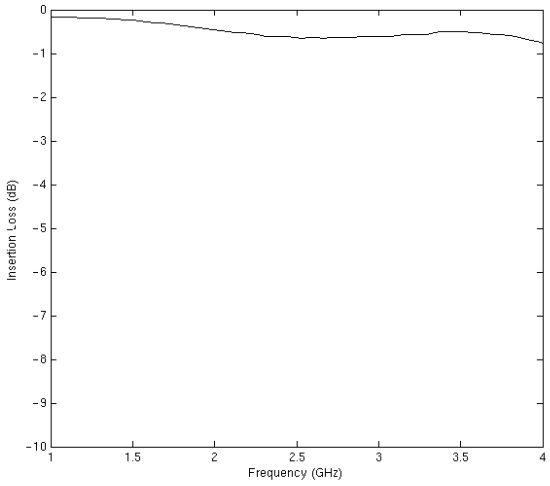

Figure 4: Measured insertion loss of the MEMS switch

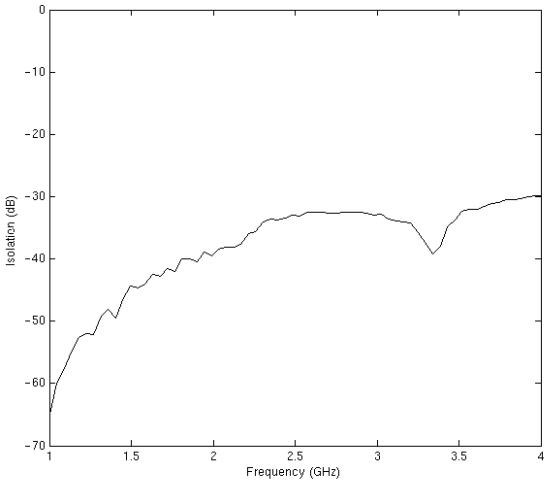

Figure 5: Measured isolation for the Magfusion MEMS switch

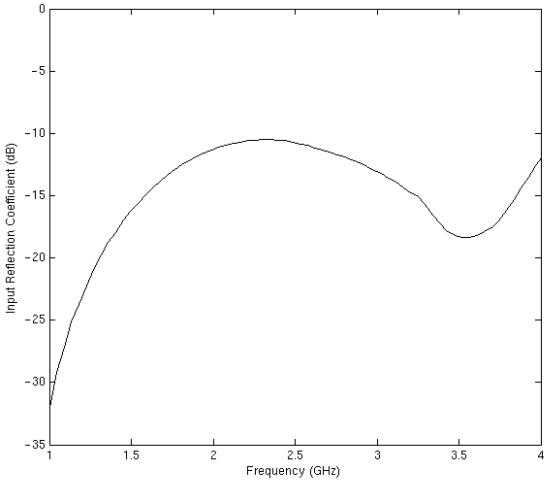

Figure 6: Measured input return loss for the Magfusion MEMS switch

4. OSCILLATOR DESIGN

Microwave oscillators are fundamental components in microwave systems that generate RF power from DC power. The design of microwave oscillators has been studied extensively and will be briefly reviewed in this section.

4.1. One-Port Negative-Resistance Oscillators

A one-port negative resistance oscillator can be illustrated by the diagram in Figure 7, which consists of a load network, $Z_L(\omega)$, and an input impedance to an active device that is dependent upon both voltage and frequency, $Z_{IN}(V, \omega)$ where

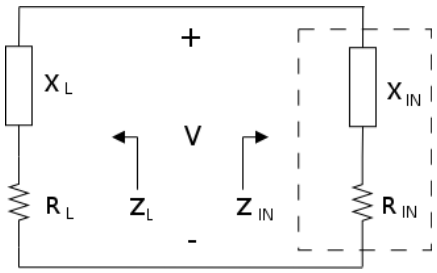

Figure 7: One-port negative resistance oscillator

$$Z_L(\omega) = R_L + jX_L(\omega)$$

and

$$Z_{IN}(V,\omega) = R_{IN}(V,\omega) + jX_{IN}(V,\omega)$$

If the circuit is oscillating then the following conditions must hold:

$$R_L + R_{IN}(V,\omega) = 0$$

and

$$X_L(\omega) + X_{IN}(V,\omega) = 0$$

so that the round trip gain is one. Since the load is a positive resistance, or $R_L > 0$, it follows that R_L must necessarily be negative in order for oscillation to occur. In this case, the active device could be an IMPATT or a Gunn diode configured to provide a negative input impedance. Another common way to express the oscillation condition is with a unity product of the reflection coefficients:

$$\Gamma_{IN}(V,\omega)\Gamma_L(\omega) = 1$$

Since $X_{IN}(V,\omega)$ is amplitude dependent, the oscillation frequency is not stable. It is shown in [9] that if the frequency dependence of $Z_{IN}(V,\omega)$ is negligible for small variations around ω_0, the condition for stable oscillation is:

$$\left(\left.\frac{\partial R_{IN}(V,\omega)}{\partial V}\right|_{V=V_0}\right)\left(\left.\frac{\partial X_L(\omega)}{\partial V}\right|_{\omega=\omega_0}\right) > 0$$

when the change in load resistance with frequency is negligible, as is usually the case.

4.2. Two-Port Negative-Resistance Oscillators

The general block diagram for a two-port negative-resistance transistor oscillator is shown in Figure 8. The terminating network is chosen to create a negative input resistance to the transistor. This is done by selecting a Z_T that is in the unstable region of the transistor. It follows

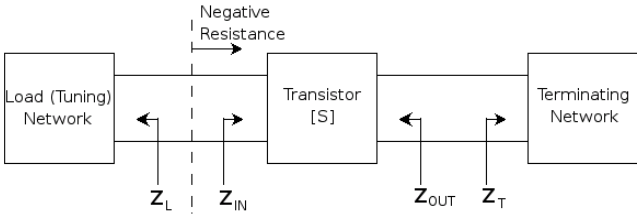

Figure 8: Two-port negative resistance transistor oscillator

then that the device used in Figure 8 must be potentially unstable at the desired oscillation frequency and biasing conditions in order for it to be used as an oscillator. A network is considered unconditionally stable if $|\Gamma_{IN}| < 1$ and $|\Gamma_{OUT}| < 1$ for all passive source and load impedances, whereas a network is conditionally stable if $|\Gamma_{IN}| < 1$ and $|\Gamma_{OUT}| < 1$ for only certain source and load impedances. Therefore, the device used in the oscillator circuit must have [10]

$$\left|\Gamma_{IN}\right| = \left|S_{11} + \frac{S_{12}S_{21}\Gamma_T}{1 - S_{22}\Gamma_T}\right| \geq 1$$

or

$$\left|\Gamma_{OUT}\right| = \left|S_{22} + \frac{S_{12}S_{21}\Gamma_L}{1 - S_{11}\Gamma_L}\right| \geq 1$$

for some Z_L or Z_T. If the device is unilateral (i.e. $S_{12} = 0$), these equations simplify the conditional stability requirements to:

$$\left|\Gamma_{IN}\right| = \left|S_{11}\right| \geq 1$$

or

$$\left|\Gamma_{OUT}\right| = \left|S_{22}\right| \geq 1$$

To determine which source and load impedances will produce instability, input and output stability circles can be drawn on a Smith chart.

For an oscillator, it is desired to have a transistor with a large degree of instability to allow for flexibility in the design of the terminating and load networks. Instability of a transistor is often enhanced through the use of series or shunt feedback. After a terminating network has been selected that provides a large negative input impedance to the device, the load impedance, Z_L, can be designed to match Z_{IN}. Since the input resistance will become less negative as the oscillations build, it is necessary to make the negative input impedance larger than the load resistance to ensure that oscillations will build and reach the desired steady-state. A commonly used design equation [10] is to make the load resistance one-third the magnitude of the negative input resistance.

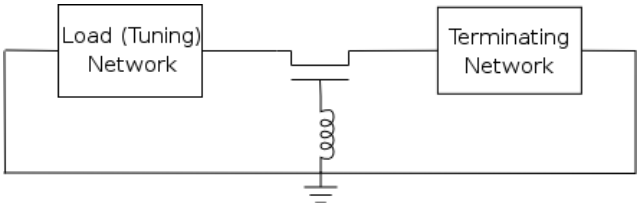

Figure 9: Common-gate transistor oscillator configuration

For the proposed FSK topology any transistor configuration can be used as long as two resonant loads can be selected independently via the MEMS switch. To demonstrate the FSK concept, a common-gate oscillator configuration was used, as shown in Figure 9. An inductor is placed between the gate and ground in order to increase the instability of the device.

5. FSK MODULATOR CIRCUIT DESIGN

An FSK modulator using the proposed concept was designed and fabricated on a microwave substrate using the MEMS SPDT switch discussed above. The FSK modulator using the common-gate oscillator topology used is shown in Figure 10. The two frequencies that the proposed modulator was designed to operate at to represent the binary data was selected to be 2.1 GHz and 2.15 GHz. The maximum data rate will be limited by the speed of the MEMS switch to approximately 3 kbps. The transistor used for the oscillator is a low-noise pseudomorphic high-electron mobility transistor (HEMT) housed in a miniature (SOT-343) plastic surface mount package manufactured by Agilent (model: ATF-33143 [11]). This device has a low-noise figure and excellent linearity and can be made unstable easily at the desired frequency of oscillation. Agilent provides data to create a die model in ADS for the device and also includes a circuit model that includes the parasitic elements associated with the packaging of the device. This model was used in all ADS simulations.

The process of designing the proposed FSK modulator essentially consists of designing two oscillator circuits using the topology of Figure 10 that share a common termination network. The substrate used for this modulator is the microwave laminate model GML 1000 produced by GIL Technologies [12]. This substrate is 0.5 mm thick and has a relative permittivity of 3.2.

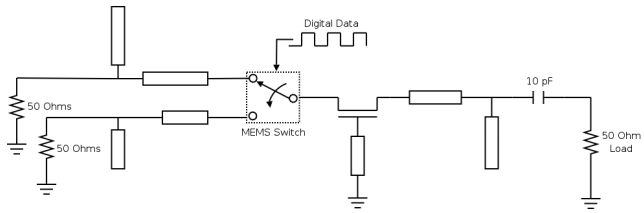

Figure 10: FSK modulator using common-gate oscillator configuration

The first step in the design is to ensure that the oscillator is potentially unstable at the desired oscillation frequencies. It was found through initial simulations that by including a 16 mm 50 Ω transmission line between the gate of the transistor and ground the instability of the device is maximized.

The output stability circles of the device can be calculated and then a terminating network can be selected that presents a large negative input impedance at the input to the device. The value of termination impedance chosen is:

$$\Gamma_T = \frac{Z_T - Z_0}{Z_T + Z_0} = 0.29\angle 157.13^o$$

or

$$Z_T = 28.30 + j6.96 \quad \Omega$$

With this termination, the input reflection coefficient and input impedance to the transistor are:

$$\Gamma_{IN} = 2.13\angle -6.71^o$$

or

$$Z_{IN} = -135.74 - j19.16 \quad \Omega$$

To create this value of termination impedance a single-stub matching network is used. A 10 pF DC blocking capacitor is also used and taken into account when designing the matching network. With this termination network, the required value of the load impedance is:

$$Z_L = -\frac{R_{IN}}{3} - jX_{IN} = 45.25 + j19.16$$

At this point in the design, the MEMS switch was assumed to be ideal and the load network is designed using a single-stub network with a 50 Ω packaged resistor. The oscillator circuit is shown in Figure 11 with the transistor package

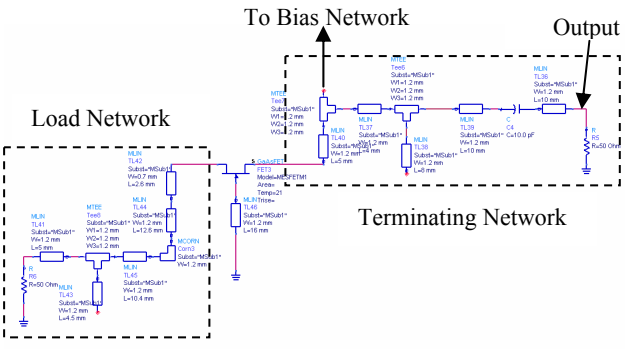

Figure 11: First oscillator circuit (biasing and transistor package model not shown)

model included, but with biasing details omitted.

Next, the second load network can be designed. The termination network (load) appears slightly different at 2.15 GHz and is given by:

$$\Gamma_T = 0.30\angle 157.45^o$$

or,

$$Z_T = 27.56 + j7.02 \quad \Omega$$

which creates an input reflection coefficient and impedance of :

$$\Gamma_{IN} = 1.53\angle -4.52^o$$
$$Z_{IN} = -232.18 - j42.05 \quad \Omega$$

Similar to the above, the load network can be created to provide oscillations at 2.15 GHz:

$$Z_L = -\frac{R_{IN}}{3} - jX_{IN} = 77.39 + j42.05 \quad \Omega$$

The final circuit including both load networks is shown in Figure 12 (biasing and transistor package model not shown for clarity). The MEMS switch is incorporated using a static SPDT ADS model with performance adjusted to match the measured performance of the MEMS switch reported above.

It is desirable for the biasing circuitry to appear as a very large impedance so that it will have little or no effect on the rest of the circuit. A combination of λ/4 transmission lines and a radial stub produces a relatively wideband large input impedance and was the bias network used for the circuit.

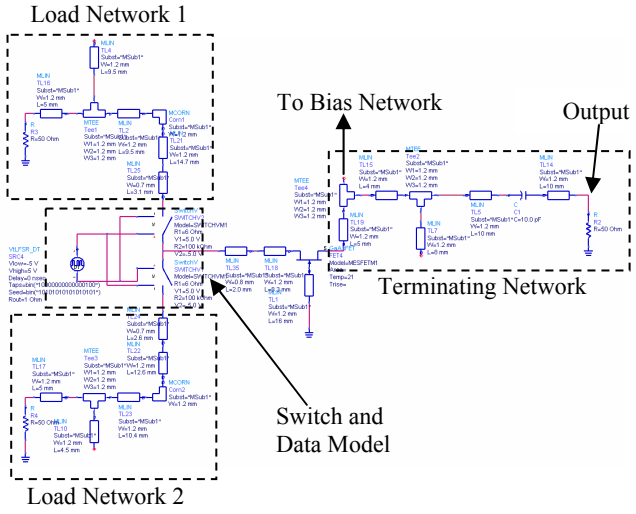

Figure 12: FSK modulator circuit (biasing details not shown)

To simulate the modulator, first the switch was held stationary in each of its two states to ensure that oscillations are occurring at the two frequencies as desired. Figure 13 shows the time-domain oscillation start-up while the switch is static in one position. As expected, the oscillations grow until they reach a steady-state.

Next, harmonic balance simulations were run with the switch in each of its two possible states. Shown in Figure 14 is the spectrum of the output when the switch is held stationary while connected to the load that produces a 2.1 GHz oscillation. The output power is shown to be approximately 5.6 dBm and exactly at 2.1 GHz. The next highest harmonic is at 6.3 GHz and is about 11 dB below the 2.1 GHz signal. With the switch in the other position, the spectrum of the output is shown in Figure 15. The strongest frequency component is clearly at 2.15 GHz at approximately 4.1 dBm. This is at least 12 dB above all other harmonics.

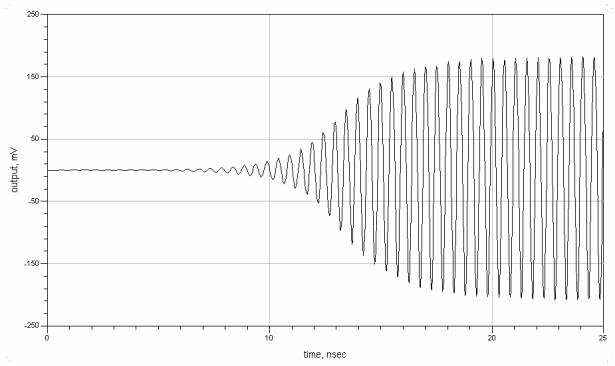

Figure 13: Oscillation start-up simulation

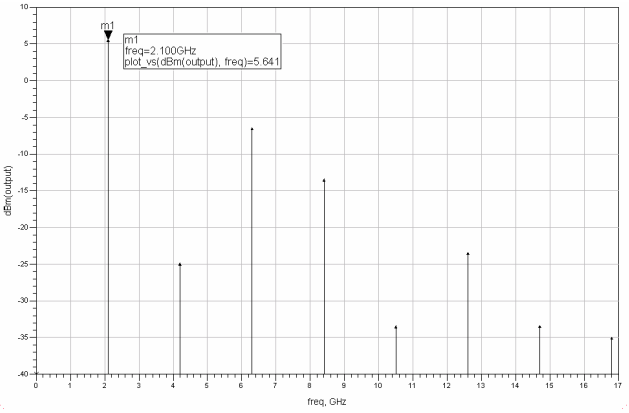

Figure 14: Spectrum of output signal while in the 2.1 GHz state

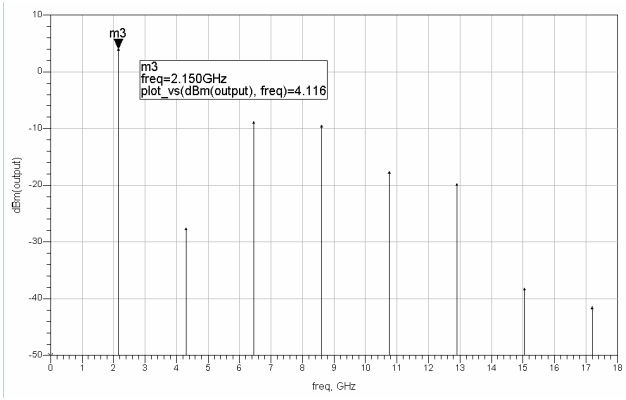

Figure 15: Spectrum of output signal while in the 2.15 GHz state

The phase noise performance was also simulated in each state of the oscillator. With the switch connected to the load that gives 2.1 GHz oscillations, the phase noise is shown in Figure 16. Figure 17 shows the phase noise while the switch is in the 2.15 GHz position. From these figures it is clear that in both states there is good phase noise performance with approximately -131 dBc and -118 dBc at a 1 MHz offset for both oscillation states.

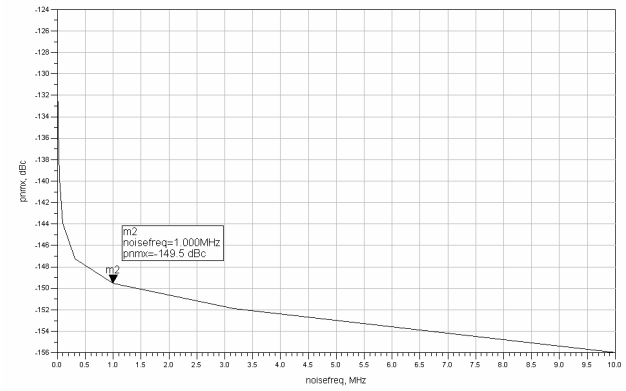

Figure 16: Phase noise performance while in the 2.1 GHz state

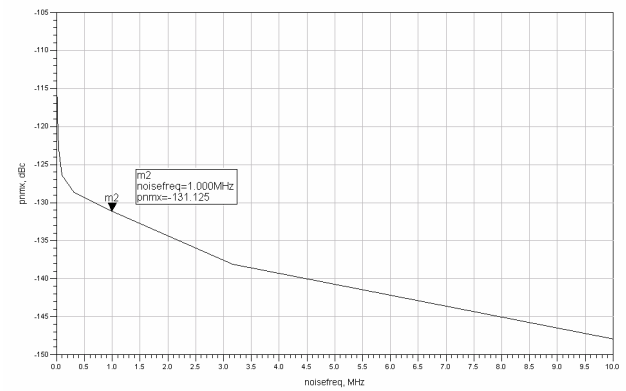

Figure 17: Phase noise performance while in the 2.15 GHz state

Due to the very large difference in the carrier frequencies and the data rate, dynamic simulations with random data sequences cannot be performed at data rates that are attainable with the MEMS switch used. The proposed FSK modulator requires a low-data rate not only because of the relatively slow speed of the MEMS switch, but also because the oscillations need time to settle into a new steady-state when the switch changes positions. If the data, and therefore the switch, are changing too rapidly there will not be time for the oscillator to settle and the modulator will not operate properly. This creates a challenge when simulating the spectrum of this FSK modulator. If a low data-rate is used then the simulations will require too much computing capabilities, but if a high data-rate is used the spectrum will not be representative of the expected FSK signal because the oscillations do not have time to settle in each state. However, since the oscillation frequency can clearly be seen to change with the state of the switch, the principal behind the FSK modulator has been demonstrated in simulations.

7. FSK MODULATOR TEST AND MEASUREMENT

The proposed FSK modulator was fabricated with a printed circuit board milling machine. The transistor, resistors, capacitor, and MEMS switch were all fixed to the PCB using conductive epoxy. A photograph of the modulator circuit is shown in Figure 18. The dimensions of the circuit board are 58 mm X 64 mm.

An Anritsu universal test fixture was used (model 3680-20) to connect to the output trace on the circuit board. The coaxial connection on the test fixture can then be used to connect the output to a spectrum analyzer.

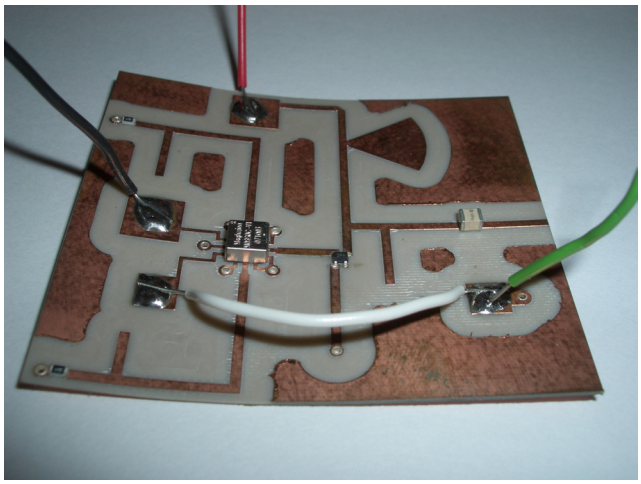

Figure 18: Photograph of fabricated FSK modulator circuit board

The spectrum analyzer used was a Rhode & Schwarz FS300 with a maximum operational frequency of 3 GHz. The spectrum while the switch is held constant in a fixed state is shown in Figure 19. The centre frequency of the spectrum analyzer is 1.8 GHz and the frequency span is 100 MHz. It is clear that oscillations are occurring at 1.8 GHz, which is lower than simulations predicted. Also, the output power is at 9.9 dBm which is higher than simulations showed. When the switch is actuated to its other state, the spectrum of the output is as shown in Figure 20 with a centre frequency approximately 1.9 GHz and again a frequency span is 100 MHz. Again, oscillations are clearly occurring, but at a frequency of 1.9 GHz. The output power is also higher than in simulations at 8.45 dBm. Furthermore, the separation between frequencies was designed and simulated to be 50 MHz and in experiment it is 100 MHz. This discrepancy is predominately due to incomplete knowledge of the transistor characteristics and the non-linearity of the transistor parameters used. Transistor parameters for simulations are generally provided by manufacturers, but they rarely include all of the information that could be used in the model. Nevertheless, the concept behind the circuit has been experimentally verified with the oscillation frequency being switched between two values based on the state of the MEMS switch.

The phase noise of the output in both possible oscillation states was measured to be -99 dBc for the 1.8 GHz signal and -98 dBc for the 1.9 GHz signal at an offset of 1 MHz. This is higher than simulations showed, but still reasonably good for the type of resonators used. A Hewlett Packard spectrum analyzer (model: 8593E) that can show signals up to 26.5 GHz was also used to view the behaviour of the higher-order harmonics. While in the 1.8 GHz oscillation state, the harmonic with the highest power was measured to be at 3.6 GHz with a power of -13.3 dBm. This is over 23 dB below the fundamental, which is very good, and in fact, better than simulations. The highest-powered harmonic while the circuit is in the 1.9 GHz state is at 9.5 GHz where the power was -23.5 dBm. This is approximately 32 dB below the fundamental, which is an excellent level of suppression of the harmonics.

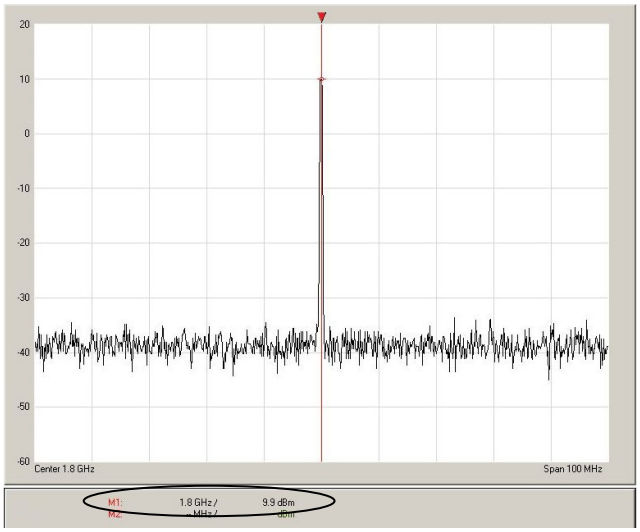

Figure 19: Measured spectrum of output in the 1.8 GHz state

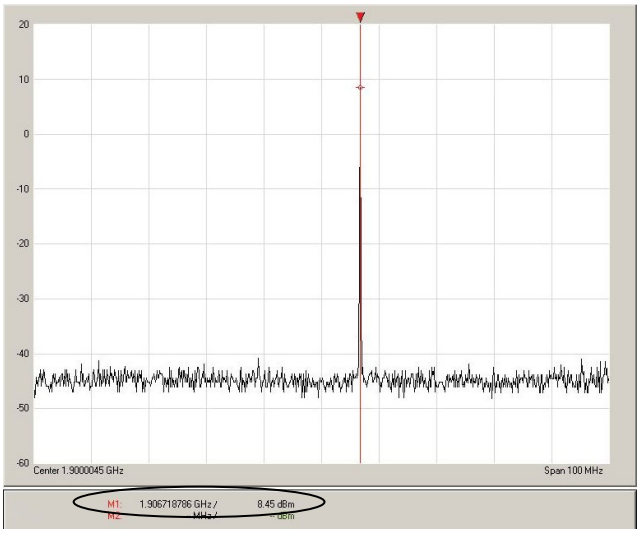

Figure 20: Measured spectrum of output in the 1.9 GHz state

The power consumption for the oscillator circuit is 17 mA x 2.5 V = 42.5 mW. This is in addition to the power consumed by the MEMS switch, which can be somewhat high depending on the data rate and format. If a different MEMS switch is used, such as an electrostatically actuated one, then the power consumption of the switch would be negligible. Alternatively, if the Magfusion switch from this work is to be used, the bit stream can be modified to significantly reduce power consumption by implementing a form of return-to-zero data which will prevent current from constantly flowing through the coil on the MEMS switch.

8. CONCLUSION

A new FSK modulator has been designed and tested that uses a MEMS switch to select between one of two possible resonant networks corresponding to a digital data signal. A packaged commercially available magnetically actuated MEMS single-pole double-throw switch was used that has a relatively low actuation voltage of ±5 V, making it easily incorporated with other electronic components. The circuit was measured to have a 1.8 GHz oscillation frequency while the switch is in one state, and a 1.9 GHz oscillation frequency when actuated to the other state. The

output power in the 1.8 GHz state is 9.9 dBm and the phase noise at a 1 MHz offset is -99 dBc. In the 1.9 GHz state, the output power is 8.45 dBm and the phase noise at a 1 MHz offset is -98 dBc. Advantages of this topology include ease of design and the ability to have resonators with significantly different resonant frequencies. This topology could be implemented monolithically and with any type of resonator. Lastly, an electrostatically actuated MEMS switch could also be used to essentially eliminate the power consumption of the switch.

9. REFERENCES

[1] C. T.-C. Nguyen, "Micromechanical Circuits for Communications Transceivers," *IEEE Bipola/BiCMOS Circuits and Technology Meeting,* pp. 142-149, 2000.

[2] A. Abbaspour-Tamijani, L. Dussopt, G. M. Rebeiz, "Miniature and Tunable Filters using MEMS Capacitors," *IEEE Trans. Microwave Theory Tech.,* Vol. 51, No. 7, pp. 1878-1884, July 2003.

[3] Y. J. Ko, J. Y. Park, J. U. Bu, "Integrated RF MEMS Phase Shifters with Constant Phase Shift," *IEEE MTT-S Digest,* pp. 1489-1492, 2003.

[4] B. R. Jackson and C. E. Saavedra, "2.4 GHz Direct-Digital Binary Phase Shift Keying Modulator using a MEMS Switch," *IEE Electronics Letters,* Vol. 40, No. 24, pp. 1539-1540, Nov. 2004.

[5] C. E. Saavedra, "Reconfigurable Bandpass Filter Structure using an SPDT MEMS Switch," *35th European Microwave Conference,* pp. 557-560, Paris, France, Oct. 2005.

[6] D. Peroulis, S. P. Pacheco, and L. P. B. Katehi, "RF MEMS Switches With Enhanced Power-Handling Capabilities," *IEEE Transactions on Microwave Theory and Techniques*, Vol. 52, No. 1, pp. 59-68, January 2004.

[7] Magfusion ML06 Datasheet available online at <http://www.magfusion.com>

[8] M. Ruan, J. Shen, and C. B. Wheeler,"Latching Micromagnetic Relays," *Journal of Microelectromechanical Systems*, Vol. 10, No. 4, pp. 511-517, December 2001.

[9] G. Gonzalez, "Microwave Transistor Amplifiers: Analysis and Design," Prentice-Hall, N. J., 1984.

[10] D. M. Pozar, "Microwave Engineering," Second Edition, John Wiley & Sons, Toronto, 1998.

[11] Agilient PHEMT model ATF-33143 Datasheet <http://cp.literature.agilent.com/litweb/pdf/5989-1917EN.pdf>

[12] GIL Technologies, GML 1000 Microwave laminate <http://www.gilam.com/GIL_Products/gml1000.htm>